https://doi.org/10.5194/essd-2022-463
Preprint. Discussion started: 14 February 2023

Open Access Earth System Science Data Discussions

High-resolution global map of closed-canopy coconut

Adrià Descals[1], Serge Wich[2], Zoltan Szantoi[3,4], Matthew J. Struebig[5], Rona Dennis[6], Zoe Hatton[2], Thina Ariffin[6], Nabillah Unus[6], David L.A. Gaveau[7], and Erik Meijaard[6]

[1]CREAF, Cerdanyola del Vallès, Barcelona 08193, Spain
[2]School of Biological and Environmental Sciences, Liverpool John Moores University, Liverpool L3 3AF, United Kingdom
[3]Science, Applications & Climate Department, European Space Agency, Frascati 00044, Italy
[4]Stellenbosch University, Stellenbosch 7602, South Africa
[5]Durrell Institute of Conservation and Ecology, University of Kent, Canterbury, England, United Kingdom
[6]Borneo Futures, Bandar Seri Begawan, Brunei Darussalam
[7]TheTreeMap; Bagadou Bas, Martel 46600, France

Correspondence to: Adrià Descals (a.descals@creaf.uab.cat)

Abstract. Vegetable oil crops cover over half of global agricultural land and have varying environmental and socioeconomic impacts. Demand for coconut oil is expected to rise, but the global distribution of coconut is understudied, which hinders the discussion of its impacts. Here, we present the first 20-meter global coconut layer, produced using deep learning for semantic segmentation, specifically a U-Net model that was trained using annual Sentinel-1 and Sentinel-2 composites from 2020. Results confirmed the feasibility of using Sentinel-1 for mapping palm species that present full canopy closure. The overall accuracy was 99.10 ± 0.20 %, which was significantly higher than the no-information rate. The producer's accuracy was 72.07 ± 22.83 % when only closed-canopy coconut was considered in the validation, but decreased to 12.34 ± 2.60 % when sparse and open-canopy coconut areas were considered, indicating that this planting context remains difficult to map with accuracy. We report a global coconut area of 12.31 ± 3.83 x 10^6 ha for dense open- and closed-canopy coconut, but the estimate is three times larger (36.72 ± 7.62 x 10^6 ha) when sparse coconut is included in the area estimation. This large area of sparse and dense open-canopy coconut is important as it indicates that production increases can likely be achieved on the existing lands allocated to coconut. The Philippines, Indonesia, and India account for most of the global coconut area, or about 82 % of the total mapped area. Our study provides the high-resolution, quantitative, and precise data necessary for assessing the relationships between vegetable oil production and the synergies and trade-offs between various sustainable development goal indicators. The global coconut layer is available at https://doi.org/10.5281/zenodo.7453178 (Descals, 2022).

https://doi.org/10.5194/essd-2022-463
Preprint. Discussion started: 14 February 2023

Open Access Earth System Science Data Discussions

1 Introduction

Vegetable oil crops (including maize) take up 65 % of all agricultural land and are particularly problematic because demand for vegetable oils is expected to nearly double in the next three decades (Meijaard et al., 2020b). Coconut (*Cocos nucifera* L.) produces about 1.7% of the global volume of vegetable oils (USDA, 2022) as well as copra, coconut water, and coconut milk. Coconut is generally overlooked in discussions about vegetable oil impacts and not many see this palm as a threat to biodiversity. However, a recent study identified coconut as a potential threat to tropical species, many of which are highly threatened and restricted to tropical islands where coconut is extensively grown (Meijaard et al., 2020a). In some of these islands, coconut is considered an invasive species that drives near-complete ecosystem state change when it becomes dominant (Young et al., 2017).

Despite the potential impacts, the coconut distribution is poorly documented except for national-level statistics on estimated harvest areas (FAO, 2022), or local-level crop mapping studies (e.g., Palaniswami et al., 2006). This may be because coconut is mostly grown in smallholdings under 4 ha (Omont, 2001) and is often intercropped, making its mapping difficult. A high-resolution global map of the distribution of coconut would serve as a basis for understanding their impacts, as well as help to shape environmental and biodiversity policy. Research is therefore needed to map coconut on a global scale, especially using high spatial resolution satellite data.

The canopy structure of palm-like trees, such as coconut, produces a distinctive backscatter response in synthetic aperture radar (SAR) (Miettinen and Liew, 2011). This characteristic response in radar data makes it possible to map palm species with closed canopies. In particular, the Sentinel-1 C-band backscatter response in palm species is characterized by low vertical transmit and vertical receive (VV) and high vertical transmit and horizontal receive (VH). Previous studies have used radar and optical satellite data for mapping closed-canopy oil palm stands (Danylo et al., 2021; Gaveau et al., 2022; Descals et al., 2021). Coconut mapping has received less attention than oil palm, and previous studies have focused only on the local and regional scale (Lang et al., 2021; Jenifer and Natarajan, 2021). Moreover, despite efforts to map oil palm, it is still unclear how well Sentinel-1 can differentiate between oil palm, coconut, and other palm species.

The aim of this study was to produce the first global coconut map at high spatial resolution (20 meters) and estimate the global coconut area using satellite remote sensing. To achieve this aim, we first identified potential areas where climate was favourable for coconut growth. We then used a semantic segmentation model that classified Sentinel-1 and Sentinel-2 annual composites from 2020. Finally, we employed a sampling-based approach to validate the results.

https://doi.org/10.5194/essd-2022-463
Preprint. Discussion started: 14 February 2023

2 Methods

2.1 Bioclimatic analysis

We identified potential coconut-growing regions and classified satellite data in these areas. First, we conducted a literature search to identify the coconut-producing regions of the world. Next, we visually inspected imagery with sub-meter resolution and collected points at locations where we identified coconut (Fig. 1a). The points were collected in coconut-producing regions, based on our literature search, and coconut regions according to the SPAM model (Yu et al., 2020). Three interpreters visualized sub-meter resolution and collected at least five points in each SPAM grid cell (5-arcmin grid). Coconut can be distinguished from other palm species in sub-meter satellite images (Fig. 2). These sub-meter-resolution satellite images are displayed in the base layer of Google Earth. If available, the interpreters visualized images from Google Street Maps to verify the presence of coconut. Once all coconut-producing regions were sampled, we extracted the bioclimatic values from the WorldClim V1 Bioclim (Hijmans et al., 2005) in the collected points. WorldClim V1 Bioclim consists of 19 bioclimatic variables derived from monthly temperature and precipitation. We used the version of the product with a spatial resolution of 30 arcsec. The distribution of values outlined the range of bioclimatic values for coconut, and we used this range of values to generate the potential coconut distribution map; a pixel in the WorldClim dataset was considered suitable for coconut growth if at least 18 of the 19 bioclimatic variables fell within the bioclimatic range.

2.2 Sentinel-1 and Sentinel-2 compositing

Sentinel-1 and Sentinel-2 annual composites for the year 2020 were the input data of the classification model. Sentinel-1 consists of two SAR satellites with a 6-day revisit time (Torres et al., 2012). We used the polarization bands VV and VH, and the median was computed for all available observations in the ascending and descending scenes separately. The annual composite of Sentinel-1 was the mean of the two orbit composites for 2020. Sentinel-2 consists of two optical satellites that provide images at a revisit time of 5 days. We used the Sentinel-2 level-2A product, which contains terrain-corrected top-of-canopy reflectance. Non-valid observations were masked using the Scene Classification Layer, which is produced by the ATCOR algorithm for the level-2A product (Drusch et al., 2012). The Sentinel-2 annual composites were generated using the median of all available valid observations for 2020. The compositing for Sentinel-1 and Sentinel-2 was identical to that of the global oil palm layer described in Descals et al. (2021), with the exception that the global oil palm layer was created with images from the second half of 2019 rather than the entire 2020. Coconut is an evergreen plant and its canopy does not show substantial seasonal changes that can be captured in Sentinel-1 and Sentinel-2. The annual compositing used in this study may not be effective for mapping crops and vegetation that present a distinctive land surface phenology, which can be key information for successfully mapping their extent (Son et al., 2013).

https://doi.org/10.5194/essd-2022-463
Preprint. Discussion started: 14 February 2023

2.3 Feature selection

The coconut classification follows a methodology similar to that used for the global oil palm layer (Descals et al., 2021). The classification comprised a semantic segmentation model that used three input layers. Two of these layers were the VV and VH polarization bands from Sentinel-1, owing to the capabilities of SAR data for mapping palm plantations (Descals et al., 2019). The optical band 4 from Sentinel-2 (red band; wavelength centred at 665 nm) was the third input layer in the global oil palm layer. Band 4 was chosen because it is the 10-meter resolution band that provided the clearest depiction of harvesting trails in industrial plantations. In the red spectrum, harvesting trails have a high reflectance that contrasts with the low reflectance of the surrounding oil palm.

In contrast to oil palm, coconut plantations do not present a harvesting road network that can be identified in 10-meter satellite data. Extensive coconut plantations, such as those found in Tabou (Côte d'Ivoire) and in small islands such as Talina (Solomon Islands) or Mapun (Philippines), generally lack harvesting roads that are visible in Sentinel-1 and Sentinel-2. In addition, there were coconut plantations incorrectly classified as oil palm in the global oil palm layer (Descals et al., 2021), indicating that a spectral band other than band 4 could better distinguish oil palm from coconut. Thus, we inspected the spectral separability between oil palm and coconut plantations for all 10- and 20-meter Sentinel-2 bands. To test the spectral separability, we collected 40 points distributed in oil palm and 40 points in coconut plantations in Riau and Jambi provinces (Indonesia). These provinces have a high density of both oil palm and coconut plantations. We normalized the Sentinel-1 and -2 bands using the z-normalization and evaluated the separability using the one-dimensional Bhattacharyya distance (Theodoridis and Koutroumbas, 2006). The Bhattacharyya distance evaluates the overlap between two independent distributions; the higher the Bhattacharyya distance, the lower the overlap between the spectral values of oil palm and coconut. The Sentinel-2 band that presented the highest spectral separability was used as the optical band in the classification model.

2.4 Semantic segmentation

The Sentinel-1 and Sentinel-2 composites were classified using a semantic segmentation model, specifically a U-Net model with the MobileNetv2 as backbone (Falk et al., 2019). Semantic segmentation consists of a pixel-wise classification of an image using convolutional neural networks. Deep learning models using convolutional neural networks can automatically capture the spatial and contextual information in the image and, as a result, less effort is required compared to feature engineering in standard machine learning (Ma et al., 2019). Semantic segmentation models have been used for oil palm mapping at the global scale (Descals et al., 2021) and coconut mapping at the regional scale (Jenifer and Natarajan, 2021).

Semantic segmentation models require image data with a fixed size for both training and prediction. We set the size of the input images to 512×512 pixels, which is approximately 10×10 km in a 20-meter resolution image. The collection of

https://doi.org/10.5194/essd-2022-463
Preprint. Discussion started: 14 February 2023

training data consisted of digitizing polygons in the coconut-producing regions that were identified during the bioclimatic analysis. The polygons were drawn in 146 training images (Fig. 1b) using the sub-meter resolution images that are displayed as the base layer in Google Earth to discriminate coconut from other land covers. The U-Net consisted of a binary classification of coconut (digitized polygons) and the rest of land covers (image background) and, thus, the resulting layer was a binary raster, in which each pixel presented values of 0 (coconut is not present) and 1 (coconut is present). The U-net model was trained and deployed using the PyTorch framework in the Microsoft Planetary Computer hub.

2.5 Validation

To measure the errors in the maps, we needed extensive randomly distributed, well-characterised reference sites across the coconut producing region. We evaluated the accuracy of the global coconut layer using the good practices for estimating area and assessing accuracy as described by Olofsson et al. (2014). We used stratified random sampling over the areas delimited in the potential coconut distribution. A total of 10,200 reference points were sampled: 557 points in pixels classified as 'coconut' and 9,643 points in pixels classified as 'other'. In the stratified random sampling, the pixels that present the same class have an equal probability of being sampled. Here, we sought a cost-effective alternative by visually reviewing the sub-meter resolution images from Google Earth because coconut is easily identified using such data. If images from Google Street Maps were available, the interpreters visualized the images to verify the presence of coconut. The interpreters assigned a 'truth' label out of the following 5 interpretations:

0. Land cover could not be determined because high resolution data was not available.
1. Other land cover. Coconut is not present within the 20-meter pixel.
2. Sparse coconut. Low density of coconut trees. There are between 1 and 4 coconut trees within the 20-meter pixel.
3. Dense open-canopy coconut. There are more than 4 coconut trees within the 20-meter pixel, but coconut trees do not reach the full canopy closure.
4. Closed-canopy coconut. There are more than 4 coconut trees within the 20-meter pixel and coconut trees fully cover the ground.

The validation points were first labelled by a team of three interpreters and, then, we used a second level of verification (Szantoi et al., 2021). The second level of verification consisted of an independent interpreter that verified the points that the team labelled as 'coconut'. There were 1,814 points in which the land cover could not be determined and, thus, the total number of reference points was 10,186 in the accuracy assessment (Fig. 1c). The number of points were 7,581 for 'other land cover', 164 for 'sparse coconut', 120 for 'dense open-canopy coconut', and 202 for 'closed-canopy coconut'. In the accuracy assessment, the points labelled as 'other land cover' were recoded as 0 (class 'other'). For the class 'coconut', we considered three definitions (Fig. 2a). The first definition considered class 'coconut' when a coconut tree was found within a 20-meter pixel. Points labelled as 'sparse coconut', 'dense open-canopy coconut', and 'closed-canopy coconut' were recoded as 1.

https://doi.org/10.5194/essd-2022-463
Preprint. Discussion started: 14 February 2023

This initial definition aimed to provide an estimate of all coconut-growing regions. The second definition considered class 'coconut' the points labelled as 'dense open-canopy coconut' and 'closed-canopy coconut'. This second definition aimed to evaluate the capability of Sentinel-1 and -2 for mapping dense coconut stands that do not reach the full canopy closure. The third definition only considered points labelled as 'closed-canopy coconut trees' as class 'coconut'.

The accuracy metrics included the producer's accuracy (PA), the user's accuracy (UA), and the overall accuracy (OA). The producer's accuracy indicates the proportion of pixels of a given class that were not omitted in the classification, while the user's accuracy shows the proportion of pixels that were not committed for a given class. The OA represents the proportion of pixels that were correctly classified. We also tested whether the OA was significantly higher than the no-information rate. The no-information rate is the overall accuracy obtained by classifying all pixels with the largest land cover class —in our case, the class 'Other'. An overall accuracy significantly higher than the no-information rate indicates that the segmentation model did better than classifying indiscriminately all pixels with the class 'Other'. We reported the post-stratified metrics for PA, UA, and OA using the practices in Olofsson et al. (2014) and Szantoi et al. (2021). These practices also explain the area estimation for each class in the land cover map. While the mapped area reveals the area that was classified as a particular class, the area estimates account for omission and commission errors and provide an area with a confidence interval. All metrics of accuracy and area estimates were reported with a confidence interval of 95 %.

2.6 Area estimates in small tropical islands

The global coconut layer relies on the availability of Sentinel-1 and Sentinel-2 data. These two satellites provide images for the larger land bodies across the globe, but the data is missing in parts of the Pacific and other small tropical islands. On small islands with no Sentinel-1 or Sentinel-2 data, coconut mapping was not possible using our classification model. To overcome this issue, we used a sampling-based method to estimate the coconut area in small tropical islands, owing to the availability of sub-meter resolution satellite images in most of these islands. The sampling-based approach comprised randomly sampling 5,000 points within the small tropical island extents (Fig. 1d). Small tropical islands included islands with an area between 1 to 200 ha in the tropics (latitudes within latitudes 30°S and 30°N) in a reference dataset (Sayre et al., 2019). The points were visually interpreted and categorized with the following 5 classes:

0. Land cover could not be determined because sub-meter resolution data was not available.
1. Non-vegetated land cover. Vegetation coverage is <50 % and coconut trees are not present within the 20-meter pixel.
2. Other vegetation. Vegetation coverage is >50 % and coconut trees are not present within the 20-meter pixel.
4. Sparse coconut. Low density of coconut trees; between 1 and 4 coconut trees within the 20-meter pixel.
5. Dense open-canopy and closed-canopy coconut; more than 4 coconut trees within the 20-meter pixel.

https://doi.org/10.5194/essd-2022-463
Preprint. Discussion started: 14 February 2023

Open Access Earth System Science Data Discussions

The area occupied by coconut in the small islands could be inferred using the proportion of coconut points; $Area_{coconut} = Area_{islands} \; x \; n_{coconut}/n_{total}$, where $Area_{coconut}$ is the area covered by coconut, $Area_{islands}$ is the total area of small islands per country or globally. The 95 % confidence interval for $Area_{coconut}$ was estimated using the confidence interval for a population proportion; $CI = 1.96 \; x \sqrt{p(p-1)/n}$, where CI is the confidence interval, p is the proportion of points categorized as coconut ($n_{coconut}/n_{total}$), and n is the total number of sampled points. The area estimates of small islands did not consider the difference between dense open-canopy and closed-canopy coconut. The distinction was made solely to assess the performance of the classification model for mapping dense open-canopy coconut.

3 Results

We collected 1,139 points in places where coconut was visually identified using sub-meter resolution images (Fig. 1a). The points were located in the tropics between 25.24°S and 26.40°N, generally in low-elevation areas close to the coast. The coconut trees at the highest elevation were found at 988 meters in the Indian state of Karnataka. Nevertheless, the average altitude was 101 meters and the average distance to the ocean was 750 meters. Some coconut palms were found hundreds of kilometres inland; for example, a coconut tree was found in Bolivia 808 kilometres from the Pacific Ocean (Fig. A2a). These coconut trees presented yellow-coloured leaves, indicating substandard growing conditions, and were never observed as a plantation. The bioclimatic analysis confirmed that coconut grows predominantly in regions with a warm and humid oceanic climate, characterized by low daily and seasonal temperature variations due to the proximity of oceans. The annual temperature ranged between 22.4 and 28.8 °C (Table A1). The lowest temperature recorded during the coldest month was 11.5 °C, indicating that coconut cannot tolerate cold temperatures. Interestingly, we found that coconut grows in a variety of rainfall regimes. Coconut was found in humid tropical regions as well as relatively arid regions in India and East Africa, regions with no precipitation during the driest quarter and where annual precipitation was slightly above 100 mm. The limits of the potential coconut distribution were predominantly found in arid regions (Fig. A1), such as the xeric regions in Peru, Angola, Sudan, and Australia. The total area of the potential coconut distribution covered 3,705 x 10^6 ha.

The separability analysis revealed a low separability between coconut and oil palm in the VV and VH bands (Fig. A3), which indicates that radar data may not be able to distinguish between oil palm and coconut. Among the spectral bands, Sentinel-2 band 11 (short-wave infrared spectrum; wavelength centred at 1,614 nm) exhibited the greatest spectral separability in terms of Bhattacharyya distance. Visual inspection of the VV – VH – band 11 annual composites revealed that these three bands have the potential to distinguish between oil palm, coconut, and the rest of land covers (Fig. 3). Thus, we selected band 11 as the optical band for the classification of coconut. Since band 11 has a spatial resolution of 20-meters, we aggregated the Sentinel-1 composites to 20-meters using a bilinear interpolation. As a result, the final coconut layer has a spatial resolution of 20 meters.

https://doi.org/10.5194/essd-2022-463
Preprint. Discussion started: 14 February 2023

The global oil palm map has an overall accuracy of 99.10 ± 0.20 % (intervals represent 95 % confidence), based on the post-stratified accuracy assessment of the 10,186 validation points and considering the first definitions of coconut, which includes sparse coconut, and dense open- and closed-canopy coconut. The overall accuracy was greater than the no-information rate (94.13 ± 0.51%), indicating that the classification improved upon one in which all pixels were classified as 'other'. The producer's and user's accuracy were 12.34 ± 2.60 % and 79.40 ± 3.43 % for the class 'coconut', respectively, and 99.97 ± 0.01 % and 99.13 ± 0.20 % for the class 'other' (Table 1). The low producer's accuracy for the class 'coconut' indicates that sparse and dense open-canopy coconut were largely omitted in the classification. Without considering points in sparse coconut, the producer's accuracy increased to 34.22 ± 10.77 %. If only closed-canopy coconut were considered, the producer's accuracy was 72.07 ± 22.83 % for the class 'coconut'.

According to a visual examination of sub-meter satellite images, we identified several palm tree species that were incorrectly classified as coconut (Fig. 2b), explaining the low user's accuracy for the class coconut (79.4%). We found false positives in sago and nypa palms (*Nypa fruticans* Wurmb.) in Southeast Asia and the Pacific, raffia (*Raphia taedigera* Mart.) in South America and Africa, betel (*Piper betle* L.) in India, euterpe (*Euterpe edulis* Mart.) in South America, attalea (*Attalea spp.* Kunth) in Central America, and palmyra (*Borassus aethiopum* Mart.) specifically in Africa. Even though band 11 was included in the classification model, oil palm plantations, especially smallholders, were residually detected as coconut. Most of these false positives were eliminated in the final layer by manually editing the output of the classification. The vast bulk of these palms were found apart from coconut plantations and could be identified in the high-resolution satellite data. For instance, in New Guinea, coconut trees typically cover the first kilometres from the sea, while sago covered areas farther inland (Fig. A4). We also found false positives for coconut in two non-palm plantations: cinnamon (*Cinnamomum spp.* Schaeff.) and mango. (*Mangifera spp. L.*). Cinnamon plantations were primarily located in India, particularly in the state of Gujarat. The mango plantations were located on the Pacific coast of Mexico. Removing false positives in mango plantations was problematic due to the co-occurrence of coconut and mango plantations in the landscape. In addition, we found plantations that contained both mango and coconut trees (Fig. A2b). Other intercropping settings were found with maize (*Zea mays* L.), rice (*Oryza spp.* L.), and banana (*Musa spp.* L.) (Fig. A2c, d, and e). In contrast, we did not find intercropping in closed-canopy coconut, which was generally devoid of understory aside grasslands and small shrublands (Fig. A2f and g).

Most of the validation points for the class 'coconut' fell in the three main coconut producing regions: the Philippines (115 points), Indonesia (130 points), and India (162 points). Owing to this dense sampling, we could generate separate accuracy assessments for these three countries (Table 1). The next country was Sri Lanka, with only 14 points labelled as coconut, which is insufficient for evaluating the accuracy. The accuracy assessment revealed similar omission rates for closed-canopy coconut at the country level compared to the global assessment. The producer's accuracy for the class 'coconut' was lowest

https://doi.org/10.5194/essd-2022-463
Preprint. Discussion started: 14 February 2023


Open Access Earth System Science Data Discussions

in the Philippines (70.25 ± 29.18 %), compared to Indonesia (80.03 ± 31.37 %) and India (77.23 ± 34.56 %), although the large confidence interval indicates that the difference is not significant.

The total area mapped as coconut in the global coconut layer was 5.78 x 10^6 ha (Table 2). Coconut was mainly found in India and Southeast Asia (Fig. 4), region where we also found the largest clusters of coconut plantations (Fig. 5). The area estimates revealed that coconut covers 36.72 ± 7.62 x 10^6 ha, including sparse, and dense open- and closed-canopy coconut. If only dense open- and closed-canopy coconut were considered in the accuracy assessment, the global coconut area was 12.31 ± 3.83 x 10^6 ha, which is similar to the 11.61 x 10^6 ha reported globally by FAO. The global coconut layer confirmed that the Philippines, Indonesia, and India are the primary coconut-producing regions (Fig. A5). The coconut mapped area was 1.54 x 10^6 ha in Philippines, 1.73 x 10^6 ha in Indonesia, and 1.47 x 10^6 ha in India, which together represent 82 % of the global coconut mapped area. Other hotspots of coconut production were found along the Pacific coast of Mexico, Brazil, Ghana, Côte d'Ivoire, Tanzania, Mozambique, Sri Lanka, Vietnam, Thailand, and Papua New Guinea. In some of these countries, the mapped coconut area corresponded well with FAO statistics, for instance, in Papua New Guinea, Vietnam, and Thailand. In contrast, Tanzania is the fourth largest coconut country with 0.60 x 10^6 ha according to FAO, but only 0.03 x 10^6 ha were mapped. In East Africa, coconut is sparsely planted (Fig. A2h), which could account for our likely underestimation. The coconut area estimate for Tanzania (0.52 ± 0.48 x 10^6 ha) was consistent with FAO, although the estimate has a large confidence interval due to low sampling in this country.

We found that several Pacific countries had a large coconut area in comparison to their overall land area. Papua New Guinea had the largest coconut area mapped (0.17 x 10^6 ha), followed by Vanuatu (0.6 x 10^6 ha) and Solomon Islands (0.5 x 10^6 ha). Fig. 4 also shows the availability of Sentinel-1 and Sentinel-2 data, which is lacking in many islands in the Pacific Ocean. According to sampling-based estimates in small tropical islands, the largest coconut area was found in Indonesia and Philippines (Fig. A6a), accounting for 33,798 ± 530 ha and 21,231 ± 630 ha of dense coconut and 34,944 ± 556 ha and 16,681 ± 444 ha of sparse coconut, respectively. The ratio of coconut to total area revealed that small islands in the Pacific had the highest coconut land cover relative to land area (Fig. A6b). Tuvalu had the highest percentage, with 81 % of their land covered with coconut trees. Other islands in Pacific countries presented a low proportion of coconut relative to total area, but a high proportion relative to vegetated land. In French Polynesia, the overall proportion of coconuts was only 22 %, but it comprised 50 % of all vegetated areas in the small islands.

4 Discussion

We produced the first global coconut map with a 20-metre resolution and estimated the global area of coconut using remotely sensed data for the year 2020. We demonstrated the capability of Sentinel-1 to map the global distribution of coconut by creating the first validated and global high-resolution closed-canopy coconut map, an important input into

https://doi.org/10.5194/essd-2022-463
Preprint. Discussion started: 14 February 2023

discussions of the sustainability of agriculture in general and vegetable oil crops more specifically. In doing so, we confirmed that the high backscatter values in the Sentinel-1 VH band are a characteristic common for palm species such as oil palm and coconut. Additionally, we showed that coconut and oil palm exhibit high spectral separability in Sentinel-2 band 11 (short-wave infrared spectrum; 1,614 nm). We do not know the biophysical basis for this low reflectance in coconut compared to oil palm but speculate that it may be due to a difference in the leaf water content and biomass. Nevertheless, the spectral separability seen in Band 11 was imperfect as residual coconut false positives were still occurring for oil palm, sago, and other palm species, explaining the low user's accuracy for the class coconut (79.4%). Our model was less able to detect coconut that did not reach full canopy closure, and coconut remained broadly undetected when trees were sparsely distributed throughout the land. This issue was also found in industrial plantations with a wide planting mark. A similar problem was found in the global mapping of oil palm, which reported higher omission errors in semi-wild oil palm in West Africa (Descals et al., 2021). Despite this, the omission error for closed-canopy coconut (72.07 ± 22.83 %) was similar to those obtained in the global oil palm layer, which were 75.78 ± 3.55 % for smallholders and 86.92 ± 5.12 % for industrial oil palm. This indicates that closed-canopy palm species can be mapped with a similar accuracy. This is not the case for sparse coconut and our finding of large areas of sparsely-grown coconut is important and requires further study. Our area estimates may change the current views on production area per country, with India rather than Philippines potentially being the country with the largest coconut producing areas (if sparse coconut is included). Our results also indicate that it is important to develop a clearer definition of what constitutes the "coconut" land class for global statistics such as those provided by the Food and Agriculture Organization, which currently does not seem to have a specific definition of its "coconut" land cover class.

Sub-meter resolution images could be used in future research to accurately map sparse coconut and small tropical islands where Sentinel-1 and -2 data are unavailable. Very-high-spatial resolution images (<1 meter), such as those obtained by DigitalGlobe satellites or Planet's SkySat, can be useful to detect coconut that did not reach the full canopy closure and coconut that is sparsely present over the land. Object detection models using sub-meter satellite data or drone images have previously been used for detecting individual oil palm trees (Li et al., 2018) and delineating the tree canopy (Chemura et al., 2015). Similar efforts have been made to map coconut using sub-meter resolution images (De Souza and Falcão, 2020; Vermote et al., 2020; Freudenberg et al., 2019). Deep learning using sub-meter images could complement our closed-canopy coconut and can also be useful for mapping different palm trees, including coconut, oil palm, and sago. Because of the high costs of such imagery, sub-meter resolution mapping would only be feasible in specific areas where these high-resolution data are crucial for informing planning and decision-making about land use and agricultural development.

The potential coconut distribution map confirmed previous insights about coconut growing requirements, with the potential distribution area covering most tropical coastal regions but not those with high aridity and low temperatures. Our potential distribution of coconuts coincides with the coastal areas in a similar map of potential distribution of coconut (Coppens

https://doi.org/10.5194/essd-2022-463
Preprint. Discussion started: 14 February 2023

D'Eeckenbrugge et al., 2018). Different types of soil can support the growth of coconut as long as they are well-drained (Chan and Elevitch, 2006), which explains why coconut grows in the first few kilometres of coastline in Papua, while sago dominates the landscape in inland swampy areas. This insight may help with future mapping of other palm species. Additionally, we found that coconut generally grows in low-elevation coastal regions, but we also found coconut trees in mountainous regions in India and Tanzania. We did not include areas more than 200 kilometres from the coast because we found very few coconut trees beyond that 200-kilometer threshold in our visual assessment of high-resolution images. These coconut trees were predominantly ornamental.

Our findings show that the area designated for growing sparse, open-canopy, and closed-canopy coconut ($36.72 \pm 7.62 \times 10^6$ ha) is significantly larger than the area recognized by the FAO (11.6×10^6 ha). The FAO underreports planted area because it is based on production data and yield, and it does not account for areas sparsely covered in coconut. This finding indicates that much more land has been allocated to coconut growing than previously reported, even though coconut production may not be very important on much of that land. We do not know enough about the nature of sparsely planted coconut areas to judge how productive these lands are. In areas where coconut is intercropped with other crops, overall land productivity depends on more than coconut production and could be quite high. Sparse coconut areas may also relate to old plantations with limited maintenance and low productivity, which is a known problem in the coconut industry (Peiris et al., 2001). Overall, the coconut industry is known to have a gap between potential and actual yields, which relates to the prevalence of pests and diseases, inferior varieties, out-dated agronomical practices, and the high proportion of senile palms (Alouw and Wulandari, 2020). Therefore, the large area of sparse and dense open-canopy coconut indicates that production increases can likely be achieved on the existing lands allocated to coconut production. This has environmental consequences because demand for coconut products is rapidly growing, putting pressure on the industry to expand land holdings. Global coconut revenues are predicted to increase from US$ 5.7 billion in 2022 to USD 7.4 billion in 2027 (MarketsandMarkets, 2022), and the more production increases can be met on existing land, the less impact this will have on food security and biodiversity in areas that would otherwise be displaced by new coconut. Furthermore, our map will help in predicting the likely impact of climate change on coconut productivity, such as recently determined for India (Hebbar et al., 2022). While we acknowledge that the impacts of these production predictions remain unclear, having the first high resolution map of global coconut provides a solid basis for monitoring how this crop develops. This map also allows for the quantification of the effects of coconut expansion on natural ecosystems such as tropical lowland forests, mangroves, and beach forests, which helps to inform global biodiversity and environmental policy. Such policies could focus on increasing productivity on existing coconut lands so that no new expansion is required, potentially focusing on sparse and open coconut regions where yield increases might be less challenging. On the other hand, meeting coconut production increases on existing dense coconut land could also allow for phasing out unproductive sparse coconut lands and restoring them to natural ecosystems with potential biodiversity and other environmental benefits (Carr et al., 2021).

https://doi.org/10.5194/essd-2022-463
Preprint. Discussion started: 14 February 2023

While we were unable to map coconut at high resolution on small islands in the Pacific (because of the absence of Sentinel-1 and -2 data), our area estimates confirm that coconut is a dominant species in many of these island nations, with several countries having more than half of their land area of small islands covered in coconut (Figure A6). This indicates the importance of this crop for many smallholder producers in the Pacific, who often grow this cash crop together with other crops, with coconut being the permanent crop and other crops grown when their prices are high (Feintrenie et al., 2010). Like elsewhere, these smallholder producers struggle with low coconut productivity, but this may be compensated by good yields from other crops. Where coconut is grown as a monoculture, reorganization of the coconut industry has been proposed, potentially along similar lines as palm oil production based on the model Nucleus Estate/Nucleus-Plasma concept. High coconut coverage on small islands in the Pacific and Indian Ocean and to a lesser extent Caribbean, may be a significant threat to biodiversity and other ecosystem services (Meijaard et al., 2020a), especially because coconut can be invasive in tropical islands (Young et al., 2017). More work needs to be done to map coconut areas on these islands, ideally using sub-meter resolution data where Sentinel-1 and -2 data are currently unavailable. Once such maps become available, they can provide better insight into the extent to which coconut has displaced natural ecosystems, relative coconut productivity (in areas with detailed harvest information), and potential for coconut expansion, conversion to other forms of agriculture, or restoration of natural ecosystems. Detailed and accurate spatial information is a key component in any land-use optimization planning, for coconut as well as other crops.

5 Data availability

The dataset presented in this study is freely available for download at https://doi.org/10.5281/zenodo.7453178 (Descals, 2022). The file 'GlobalCoconutLayer_2020_v1-1.zip' contains 886 raster tiles of 100x100 km in geotiff format. The raster files are the result of a convolutional neural network that classified Sentinel-1 and Sentinel-2 annual composites into a coconut layer for the year 2020. The images have a spatial resolution of 20 meters and contain two classes:

[0] Other land covers that are not coconut.

[1] Coconut.

The file 'GlobalCoconutLayer_2020_densityMap_1km_v1-1.zip' contains the 20-meter coconut classification aggregated to 1 km. The value of each pixel represents the coconut area (in squared meters) within the 1-km pixel.

The file 'Validation_points_GlobalCoconutLayer_2020_v1-1.shp' includes the 10,200 points that were used to validate the product. Each point includes the attribute 'Class', which is the class assigned by visual interpretation of sub-meter resolution images, and the attribute 'predClass', which reflects the predicted class by the convolutional neural network. The 'predClass' values are the same as the raster files:

[0] Other land covers that are not coconut.

https://doi.org/10.5194/essd-2022-463
Preprint. Discussion started: 14 February 2023

[1] Coconut.

The attribute 'Class' contains the following values:

[0] Land cover could not be determined because sub-meter resolution data was not available.

[1] Other land covers that are not coconut.

[2] Sparse coconut. Low density of coconut trees; between 1 and 4 coconut trees within the 20-meter pixel.

[3] Dense open-canopy coconut; more than 4 coconut trees within the 20-meter pixel but coconut trees do not reach the full canopy closure.

[4] Closed -canopy coconut; more than 4 coconut trees within the 20-meter pixel and coconut trees fully cover the ground.

[5] Palm species that are not coconut.

The global coconut layer and the coconut density map can be visualized online at: https://adriadescals.users.earthengine.app/view/global-coconut-layer (last access: 16 December 2022).

The Sentinel-1 SAR GRD and Sentinel-2 Level-2A used in this study are available at the Copernicus Open Access Hub: https://scihub.copernicus.eu/ (last access: 16 December 2022). We used all Sentinel-1 and Sentinel-2 images that overlapped the potential distribution of coconut for the year 2020.

The WorldClim bioclimatic variables (WorldClim V1 Bioclim) (Hijmans et al., 2005) can be accessed at https://www.worldclim.org/data/v1.4/worldclim14.html (last access: 16 December 2022).

Very high-resolution images (spatial resolution <1 m) from DigitalGlobe can be visualized in the Google Earth Engine code editor or Google Maps.

The 5 arcmin global coconut area modelled with SPAM (Yu et al., 2020) is available at https://doi.org/10.7910/DVN/PRFF8V.

The country-wide harvested area of coconut was extracted from the FAOSTAT database at http://www.fao.org/faostat/en/ (accessed on 10 March 2022) under the item 'Coconuts in shell - Crops and livestock products (Production)' (FAO, 2022).

6 Code availability

The original code of the U-Net model can be found at: https://github.com/qubvel/segmentation_models.pytorch (Iakubovskii, 2019)

https://doi.org/10.5194/essd-2022-463
Preprint. Discussion started: 14 February 2023

7 Conclusions

We focused on developing the second global high-resolution map of a vegetable oil crop. We mapped the global distribution of coconut using a deep learning model that classified satellite data (SAR, Sentinel-1, and optical, Sentinel-2) into a 20-meter land cover map depicting the extent of closed-canopy coconut. The model achieved a high accuracy for closed-canopy coconut, and the resulting coconut layer accurately depicts the regions with the highest density of coconut. The presented dataset can be integrated into the recently published Essential Agricultural Variables' "Perennial Cropland Mask" as well as fits the Food and Agricultural Organization's LCCS classification as "Cultivated and Managed Terrestrial Areas" - "Tree Crops" (Di Gregorio, 2005).

Our global coconut layer is of considerable interest to researchers and policy makers that inform the highly polarized debate about the use of vegetable oil crops (especially oil palm) to meet future demands for food, feed, biofuel, surfactants, and other oil uses. Our study provides the accurate high-resolution data required to evaluate the relationships between vegetable oil production and the synergies and trade-offs between different sustainable development goal indicators. Moreover, coconut presents a spatial overlap with high levels of threatened species, species endemism, and species richness, in tropical islands and, thus, the global coconut layer might benefit studies that evaluate the associated environmental impacts of coconut in such biodiversity hotspots.

8 Author contributions

The conceptualization for this work originated from SW, ZS, MS, and EM. AD designed the study. AD, RD, TA, and NU collected the training data and RD, ZH, TA, NU collected the reference points. AD implemented the data processing workflow and generated the figures and tables. AD, SW, ZS, and EM wrote the draft and AD, SW, ZS, MS, RD, ZH, TA, NU, DLAG, and EM were involved in the revision of the manuscript.

9 Competing interests

The authors have no conflicts of interest to declare.

10 Financial support

We acknowledge funding from the Microsoft AI for Earth program.

https://doi.org/10.5194/essd-2022-463
Preprint. Discussion started: 14 February 2023

References

Alouw, J. and Wulandari, S.: Present status and outlook of coconut development in Indonesia, in: IOP Conference Series: Earth and Environmental Science, 012035, 2020.

Carr, P., Trevail, A., Bárrios, S., Clubbe, C., Freeman, R., Koldewey, H. J., Votier, S. C., Wilkinson, T., and Nicoll, M. A.: Potential benefits to breeding seabirds of converting abandoned coconut plantations to native habitats after invasive predator eradication, Restoration Ecology, 29, e13386, 2021.

Chan, E. and Elevitch, C. R.: Cocos nucifera (coconut), Species profiles for Pacific Island agroforestry, 2, 1–27, 2006.

Chemura, A., van Duren, I., and van Leeuwen, L. M.: Determination of the age of oil palm from crown projection area detected from WorldView-2 multispectral remote sensing data: The case of Ejisu-Juaben district, Ghana, ISPRS journal of photogrammetry and remote sensing, 100, 118–127, 2015.

Coppens D'Eeckenbrugge, G., Duong, N. T. K., and Ullivari, A.: Geographic Information Systems. Chapter 2. Where we are today, 2018.

Danylo, O., Pirker, J., Lemoine, G., Ceccherini, G., See, L., McCallum, I., Kraxner, F., Achard, F., and Fritz, S.: A map of the extent and year of detection of oil palm plantations in Indonesia, Malaysia and Thailand, Scientific data, 8, 1–8, 2021.

De Souza, I. E. and Falcão, A. X.: Learning cnn filters from user-drawn image markers for coconut-tree image classification, IEEE Geoscience and Remote Sensing Letters, 2020.

Descals, A.: High-resolution global map of closed-canopy coconut v1-1, 2022.

Descals, A., Szantoi, Z., Meijaard, E., Sutikno, H., Rindanata, G., and Wich, S.: Oil palm (Elaeis guineensis) mapping with details: Smallholder versus industrial plantations and their extent in Riau, Sumatra, Remote Sensing, 11, 2590, 2019.

Descals, A., Wich, S., Meijaard, E., Gaveau, D. L., Peedell, S., and Szantoi, Z.: High-resolution global map of smallholder and industrial closed-canopy oil palm plantations, Earth System Science Data, 13, 1211–1231, 2021.

Di Gregorio, A.: Land cover classification system: classification concepts and user manual: LCCS, Food & Agriculture Org., 2005.

Drusch, M., Del Bello, U., Carlier, S., Colin, O., Fernandez, V., Gascon, F., Hoersch, B., Isola, C., Laberinti, P., Martimort, P., and others: Sentinel-2: ESA's optical high-resolution mission for GMES operational services, Remote sensing of Environment, 120, 25–36, 2012.

Falk, T., Mai, D., Bensch, R., Çiçek, Ö., Abdulkadir, A., Marrakchi, Y., Böhm, A., Deubner, J., Jäckel, Z., Seiwald, K., and others: U-Net: deep learning for cell counting, detection, and morphometry, Nature methods, 16, 67–70, 2019.

FAO: FAOSTAT statistical database, available at: http://www.fao.org/faostat/en/, last access: 16 December, 2022.

Feintrenie, L., Ollivier, J., and Enjalric, F.: How to take advantage of a new crop? The experience of Melanesian smallholders, Agroforestry systems, 79, 145–155, 2010.

Freudenberg, M., Nölke, N., Agostini, A., Urban, K., Wörgötter, F., and Kleinn, C.: Large scale palm tree detection in high resolution satellite images using U-Net, Remote Sensing, 11, 312, 2019.

https://doi.org/10.5194/essd-2022-463
Preprint. Discussion started: 14 February 2023

Gaveau, D. L., Locatelli, B., Salim, M. A., Manurung, T., Descals, A., Angelsen, A., Meijaard, E., and Sheil, D.: Slowing deforestation in Indonesia follows declining oil palm expansion and lower oil prices, PloS one, 17, e0266178, 2022.

Hebbar, K. B., Abhin, P. S., Sanjo Jose, V., Neethu, P., Santhosh, A., Shil, S., and Prasad, P. V.: Predicting the Potential Suitable Climate for Coconut (Cocos nucifera L.) Cultivation in India under Climate Change Scenarios Using the MaxEnt Model, Plants, 11, 731, 2022.

Hijmans, R. J., Cameron, S. E., Parra, J. L., Jones, P. G., and Jarvis, A.: Very high resolution interpolated climate surfaces for global land areas, International Journal of Climatology: A Journal of the Royal Meteorological Society, 25, 1965–1978, 2005.

Iakubovskii, P.: Segmentation Models Pytorch, GitHub repository, 2019.

Jenifer, A. E. and Natarajan, S.: CocoNet: a hybrid machine learning framework for coconut farm identification and its cyclonic damage assessment on bitemporal SAR images, Journal of Applied Remote Sensing, 15, 042408, 2021.

Lang, N., Schindler, K., and Wegner, J. D.: High carbon stock mapping at large scale with optical satellite imagery and spaceborne LIDAR, arXiv preprint arXiv:2107.07431, 2021.

Li, W., Dong, R., Fu, H., and Yu, L.: Large-scale oil palm tree detection from high-resolution satellite images using two-stage convolutional neural networks, Remote Sensing, 11, 11, 2018.

Ma, L., Liu, Y., Zhang, X., Ye, Y., Yin, G., and Johnson, B. A.: Deep learning in remote sensing applications: A meta-analysis and review, ISPRS journal of photogrammetry and remote sensing, 152, 166–177, 2019.

MarketsandMarkets: Coconut Oil Market by Product Type (RBD, Virgin, and Crude), Source (Dry Coconut and Wet Coconut), Application (Food & Beverages, Cosmetics & Personal Care Products, and Pharmaceuticals), Nature and Region - Global Forecast to 2027, 2022.

Meijaard, E., Abrams, J. F., Juffe-Bignoli, D., Voigt, M., and Sheil, D.: Coconut oil, conservation and the conscientious consumer, Current Biology, 30, R757–R758, 2020a.

Meijaard, E., Brooks, T. M., Carlson, K. M., Slade, E. M., Garcia-Ulloa, J., Gaveau, D. L., Lee, J. S. H., Santika, T., Juffe-Bignoli, D., Struebig, M. J., and others: The environmental impacts of palm oil in context, Nature plants, 6, 1418–1426, 2020b.

Miettinen, J. and Liew, S. C.: Separability of insular Southeast Asian woody plantation species in the 50 m resolution ALOS PALSAR mosaic product, Remote Sensing Letters, 2, 299–307, 2011.

Olofsson, P., Foody, G. M., Herold, M., Stehman, S. V., Woodcock, C. E., and Wulder, M. A.: Good practices for estimating area and assessing accuracy of land change, Remote Sensing of Environment, 148, 42–57, 2014.

Omont, H.: Information Sheet. COCONUT, 2001.

Palaniswami, C., Upadhyay, A., and Maheswarappa, H.: Spectral mixture analysis for subpixel classification of coconut, Current Science, 1706–1711, 2006.

Peiris, T., Fernando, M., and Waidayanatha, U. de S.: Factors influencing the productivity of coconut estates, CORD, 17, 34–34, 2001.

https://doi.org/10.5194/essd-2022-463
Preprint. Discussion started: 14 February 2023

Sayre, R., Noble, S., Hamann, S., Smith, R., Wright, D., Breyer, S., Butler, K., Van Graafeiland, K., Frye, C., Karagulle, D., and others: A new 30 meter resolution global shoreline vector and associated global islands database for the development of standardized ecological coastal units, Journal of Operational Oceanography, 12, S47–S56, 2019.

Son, N.-T., Chen, C.-F., Chen, C.-R., Duc, H.-N., and Chang, L.-Y.: A phenology-based classification of time-series MODIS data for rice crop monitoring in Mekong Delta, Vietnam, Remote Sensing, 6, 135–156, 2013.

Szantoi, Z., Jaffrain, G., Gallaun, H., Bielski, C., Ruf, K., Lupi, A., Miletich, P., Giroux, A.-C., Carlan, I., Croi, W., and others: Quality assurance and assessment framework for land cover maps validation in the Copernicus Hot Spot Monitoring activity, European Journal of Remote Sensing, 54, 538–557, 2021.

Theodoridis, S. and Koutroumbas, K.: Pattern recognition, Elsevier, 2006.

Torres, R., Snoeij, P., Geudtner, D., Bibby, D., Davidson, M., Attema, E., Potin, P., Rommen, B., Floury, N., Brown, M., and others: GMES Sentinel-1 mission, Remote sensing of environment, 120, 9–24, 2012.

USDA: Oil Crops Yearbook - USDA ERS. World Supply and Use of Oilseeds and Oilseed Products. Last updated: Friday, March 25, 2022, 2022.

Vermote, E. F., Skakun, S., Becker-Reshef, I., and Saito, K.: Remote sensing of coconut trees in tonga using very high spatial resolution worldview-3 data, Remote Sensing, 12, 3113, 2020.

Young, H., Miller-ter Kuile, A., McCauley, D., and Dirzo, R.: Cascading community and ecosystem consequences of introduced coconut palms (Cocos nucifera) in tropical islands, Canadian Journal of Zoology, 95, 139–148, 2017.

Yu, Q., You, L., Wood-Sichra, U., Ru, Y., Joglekar, A. K., Fritz, S., Xiong, W., Lu, M., Wu, W., and Yang, P.: A cultivated planet in 2010–Part 2: The global gridded agricultural-production maps, Earth System Science Data, 12, 3545–3572, 2020.

https://doi.org/10.5194/essd-2022-463
Preprint. Discussion started: 14 February 2023

Open Access Earth System Science Data Discussions

Table 1: Accuracy assessment of the global coconut layer for the year 2020. The accuracy metrics were estimated with 10,186 points randomly distributed in the regions where coconut can potentially grow. The accuracy metrics are reported with a 95 % confidence interval.

	Overall accuracy[1] (%)	User's accuracy Coconut[1] / Other (%)	Producer's accuracy Coconut[1] / Other (%)	Producer's accuracy Coconut[2] (%)	Producer's accuracy Coconut[3] (%)
World	99.10 ± 0.20	79.40 ± 3.43 / 99.13 ± 0.20	12.34 ± 2.60 / 99.97 ± 0.01	34.22 ± 10.77	72.07 ± 22.83
Philippines	93.85 ± 2.82	84.75 ± 6.52 / 94.12 ± 2.89	29.66 ± 10.39 / 99.53 ± 0.20	53.06 ± 21.83	70.25 ± 29.18
Indonesia	98.99 ± 0.61	85.82 ± 5.78 / 99.06 ± 0.61	33.21 ± 14.51 / 99.92 ± 0.03	58.75 ± 27.47	80.03 ± 31.37
India	95.90 ± 1.61	75.40 ± 6.19 / 96.12 ± 1.63	17.04 ± 6.05 / 99.73 ± 0.07	44.04 ± 21.66	77.23 ± 34.56

[1]Sparse, dense open-, and closed-canopy coconut

[2]Dense open- and closed-canopy coconut

[3]Closed-canopy coconut

Table 2: Coconut area mapped for 2020, harvested area obtained from FAO statistics for 2020, and area estimates for three definitions of coconut: 1) sparse, dense open-, and closed-canopy coconut, 2) dense open- and closed-canopy coconut, and 3) only closed-canopy coconut. The area estimates are reported with a 95 % confidence interval.

	Coconut area mapped (ha x 10^6)	Coconut area FAO 2020 (ha x 10^6)	Coconut area estimate[1] (ha x 10^6)	Coconut area estimate[2] (ha x 10^6)	Coconut area estimate[3] (ha x 10^6)
World	5.71	11.61	36.72 ± 7.62	12.31 ± 3.85	5.13 ± 1.65
Philippines	1.54	3.65	4.41 ± 1.53	2.29 ± 0.95	1.46 ± 0.63
Indonesia	1.73	2.77	4.38 ± 1.91	2.38 ± 1.12	1.64 ± 0.66
India	1.47	2.15	6.38 ± 2.22	2.32 ± 1.34	0.88 ± 0.13

[1]Sparse, dense open-, and closed-canopy coconut

[2]Dense open- and closed-canopy coconut

[3]Closed-canopy coconut

https://doi.org/10.5194/essd-2022-463
Preprint. Discussion started: 14 February 2023

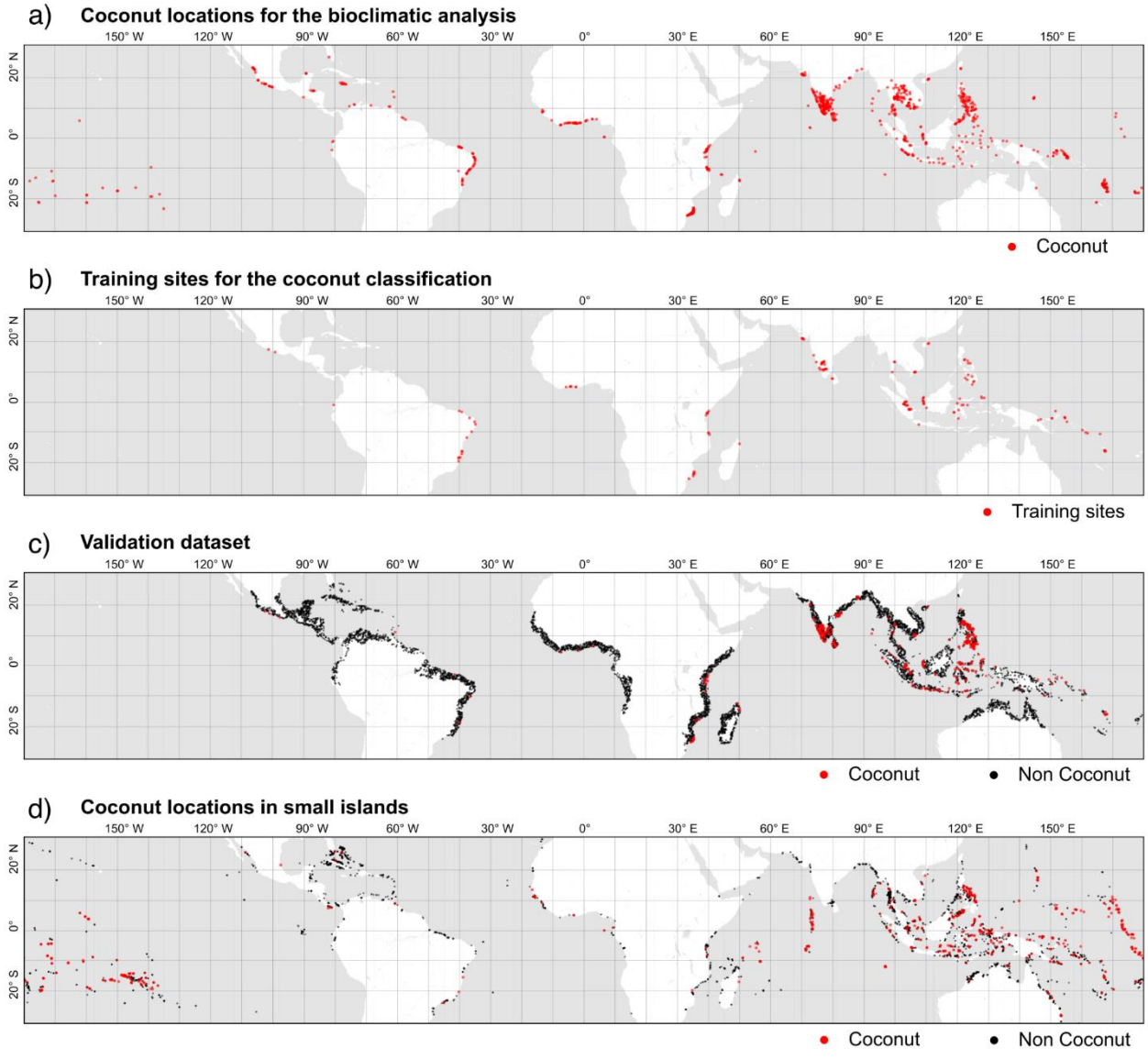

Figure 1: Four point datasets used in the methodology. (a) 1,139 points depicting coconut locations found by visual inspection of sub-meter satellite images. These points were used in a bioclimatic analysis to determine the potential distribution area of coconut. (b) Location of the 146 training sites. In these locations, Sentinel-1 and Sentinel-2 annual composites were labelled in 10x10 km for training a semantic segmentation model. (c) Validation dataset generated from a stratified random sampling. The dataset consists of 10,186 points and was used to evaluate the accuracy of the global coconut layer and estimate the global coconut area. (d) 5,000 points randomly sampled in small tropical islands (areas from 1 to 200 ha). The points were used to estimate the coconut area in small islands, where Sentinel-1 and Sentinel-2 might not be available.

https://doi.org/10.5194/essd-2022-463
Preprint. Discussion started: 14 February 2023

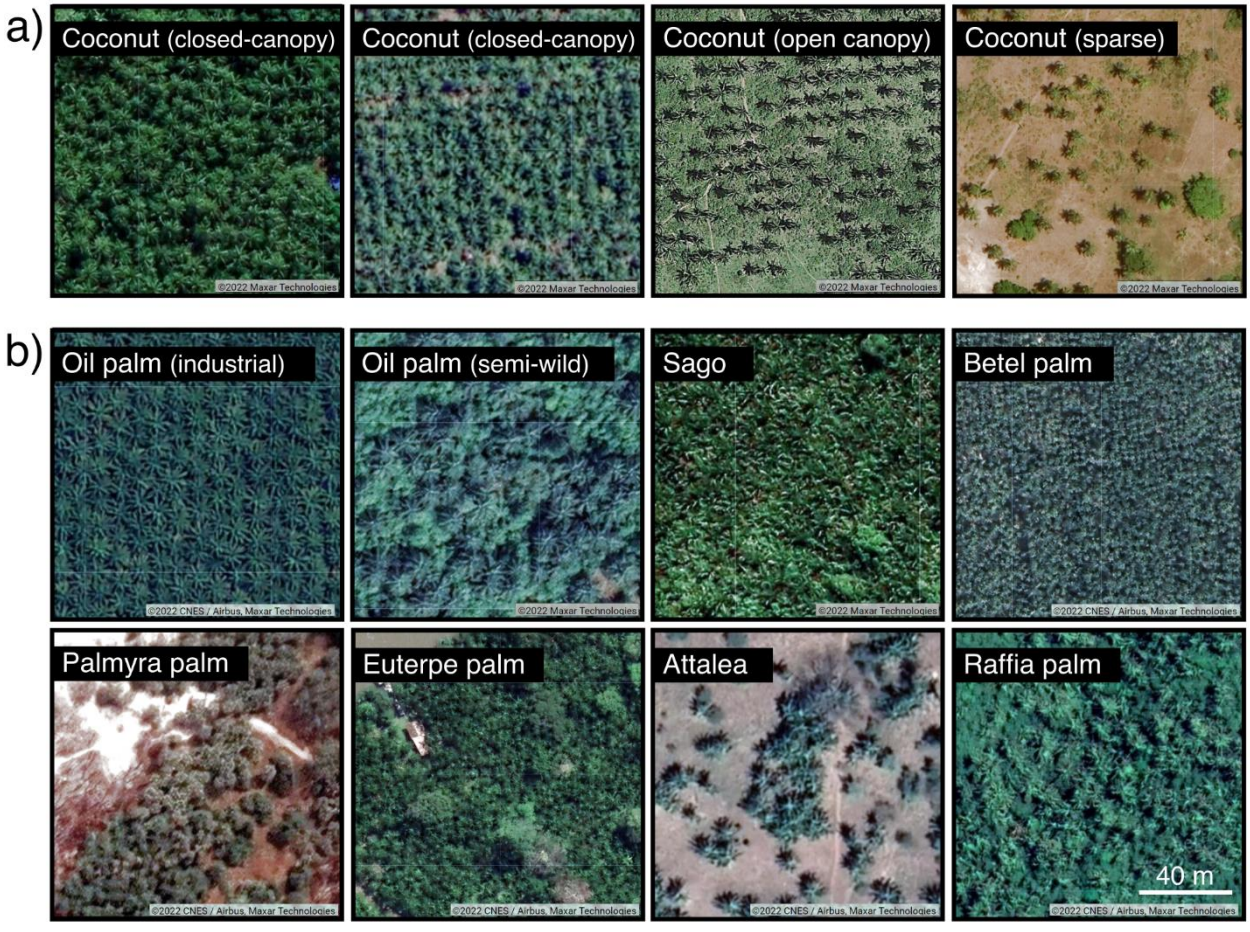

Figure 2: Sub-meter resolution images depicting (a) coconut and (b) other palm species found in the tropics. The images show (from left to right and form up to down) a closed-canopy coconut stand in Papua New Guinea (6.124043°S, 134.13848°E) and Indonesia (1.077958°N, 108.966256°E), dense open-canopy coconut in Philippines (13.792082°N, 123.016486°E), sparse coconut in Kenya (4.367173°S, 39.493028°E), industrial oil palm in Indonesia (1.123642°N, 100.498538°E), semi-wild oil palm in Nigeria (6.641218°N, 5.388639°E), sago in Papua New Guinea (6.122091°S, 134.139178°E), betel palm in India (13.980709°N, 75.632272°E), palmyra palm in Gabon (6.078832°S, 12.330894°E), euterpe palm in Brazil (1.492261°S, 48.3734988°W), attalea palm in Mexico (16.10187°N, 97.396666°W), and Raffia palm in Brazil (4.295997°S, 42.943344°W). The satellite images are the sub-meter resolution images that are displayed as the base layer in Google Earth @ Google.

https://doi.org/10.5194/essd-2022-463
Preprint. Discussion started: 14 February 2023

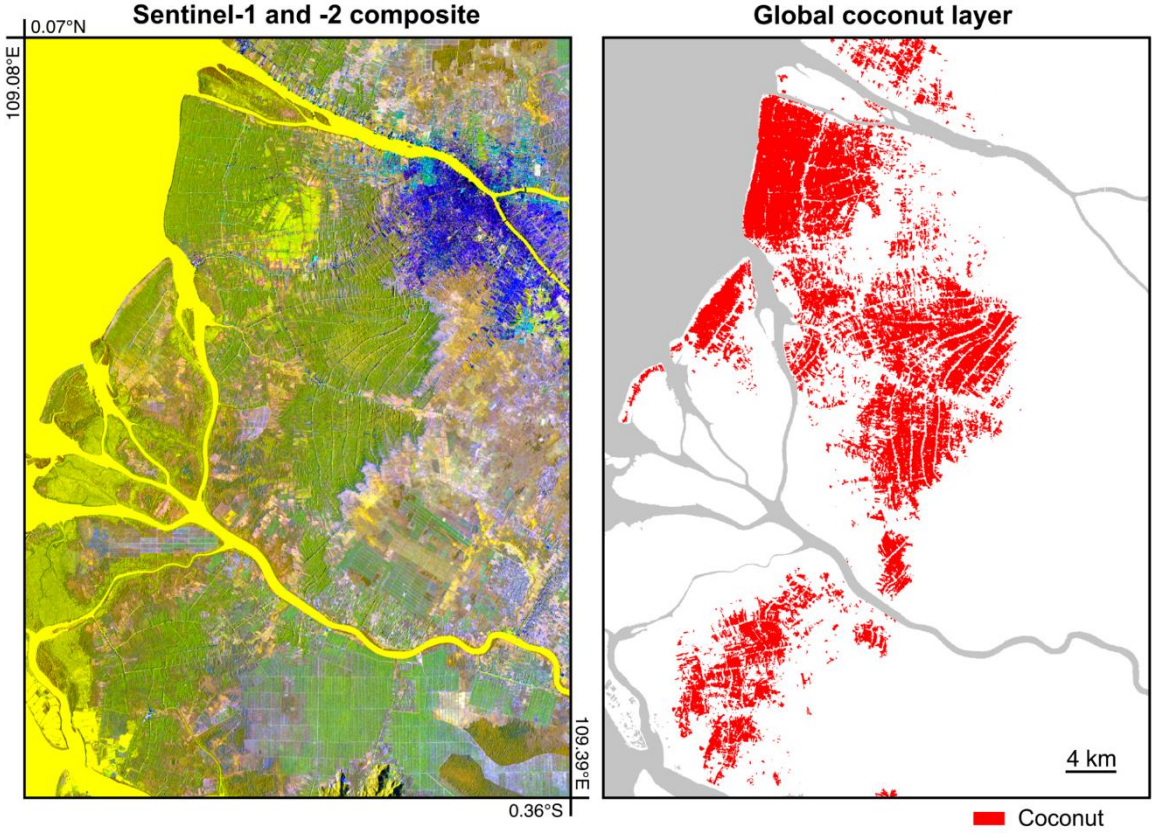

Figure 3: Classification of a Sentinel-1 and Sentinel-2 annual composite in West Kalimantan (Indonesia). The Sentinel-1 and -2 composite (left panel) includes the polarization bands VV and VH, and the spectral band 11 (short-wave infrared). In this composite, coconut and oil palm appear in different shades of green. Oil pam is present in the lower-right part of the image with a brighter green colour than coconut. In this composite, water appears in yellow. The classification image (right panel) shows the coconut plantations in red.

https://doi.org/10.5194/essd-2022-463
Preprint. Discussion started: 14 February 2023

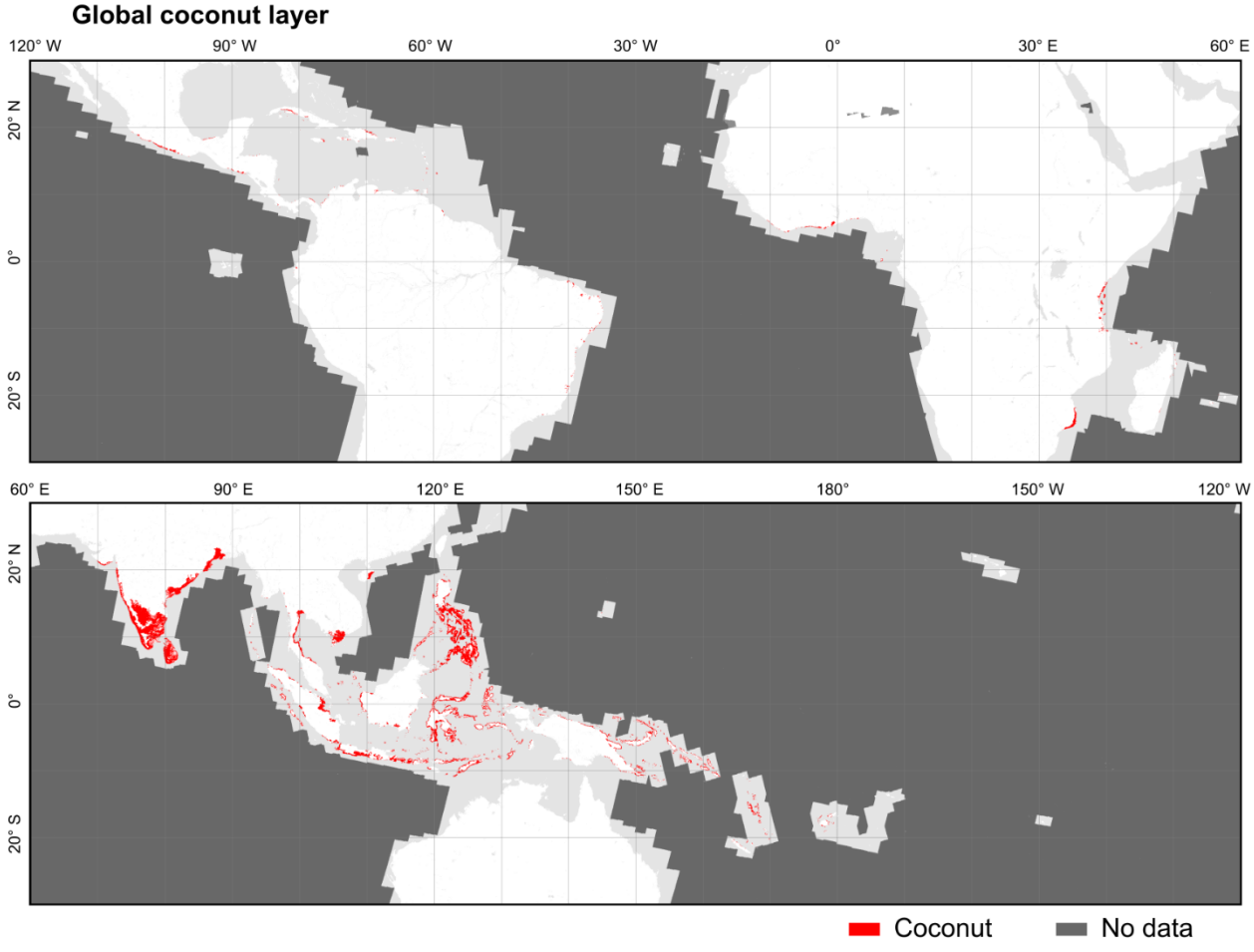

Figure 4: Global coconut layer obtained from the classification of Sentinel-1 and Sentinel-2 annual composites for the year 2020. The original global coconut layer has a 20-meter resolution but, for illustration purposes, this map was aggregated to 1 km. Red depicts 1-km pixels where at least one pixel was classified as coconut in the original 20-meter product. Dark grey represents regions where Sentinel-1 and Sentinel-2 were not available.

https://doi.org/10.5194/essd-2022-463
Preprint. Discussion started: 14 February 2023

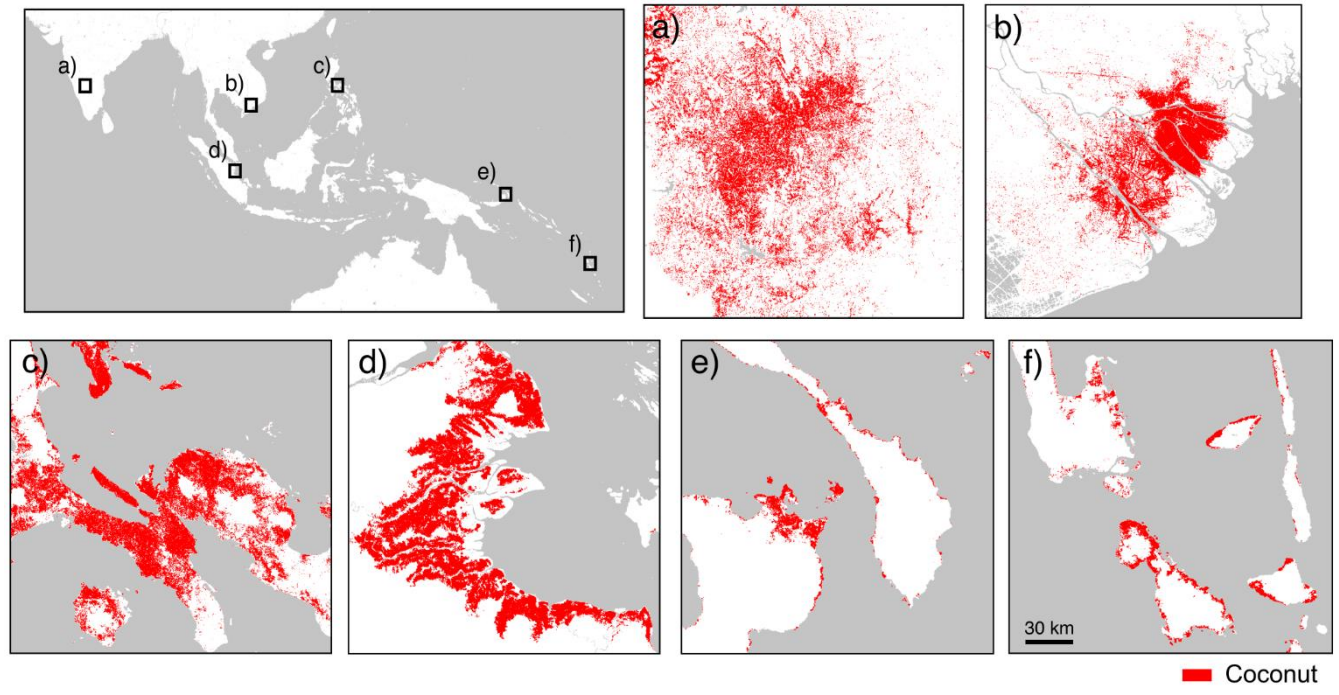

Figure 5: Detail of the global coconut layer in six coconut producing regions: a) Mysore district (India), b) Mekong delta (Vietnam), c) Quezon and Camarines provinces (Philippines), d) Riau and Jambi provinces (Indonesia), e) East New Britain and New Ireland provinces (Papua New Guinea), and f) islands of Vanuatu.

https://doi.org/10.5194/essd-2022-463
Preprint. Discussion started: 14 February 2023

Open Access Earth System Science Data Discussions

APPENDIX A

Table A1: Range of climate values extracted from 1,139 coconut locations in the world. These ranges represent the minimum and the maximum values of the 19 WorldClim bioclimatic variables, elevation, slope, and maximum distance to the sea. The variable names bio05 and bio06 represent the maximum temperature of the warmest month and the minimum temperature of the coldest month.

bioVariables	minValues	maxValues	Units
Annual mean temperature	22.4	28.8	°C
Mean diurnal range	4.1	12.2	°C
Isothermality	39.0	93.0	%
Temperature seasonality	1.1	37.8	°C
Max temperature of warmest month	28.3	37.7	°C
Min temperature of coldest month	11.5	25.1	°C
Temperature annual range (bio05-bio06)	5.4	22.3	°C
Mean temperature of wettest quarter	21.6	29.2	°C
Mean temperature of driest quarter	19.1	29.7	°C
Mean temperature of warmest quarter	23.7	31.4	°C
Mean temperature of coldest quarter	18.2	27.7	°C
Annual precipitation	108	5132	mm
Precipitation of wettest month	35	1427	mm
Precipitation of driest month	0	282	mm
Precipitation seasonality	8	165	Coef. of variation
Precipitation of wettest quarter	83	3377	mm
Precipitation of driest quarter	0	935	mm
Precipitation of warmest quarter	28	1268	mm
Precipitation of coldest quarter	0	2776	mm
Precipitation of coldest quarter	0	2776	mm
Elevation	0	988	m
Slope	0	26.4	°
Max distance to sea	0	278	km

https://doi.org/10.5194/essd-2022-463
Preprint. Discussion started: 14 February 2023

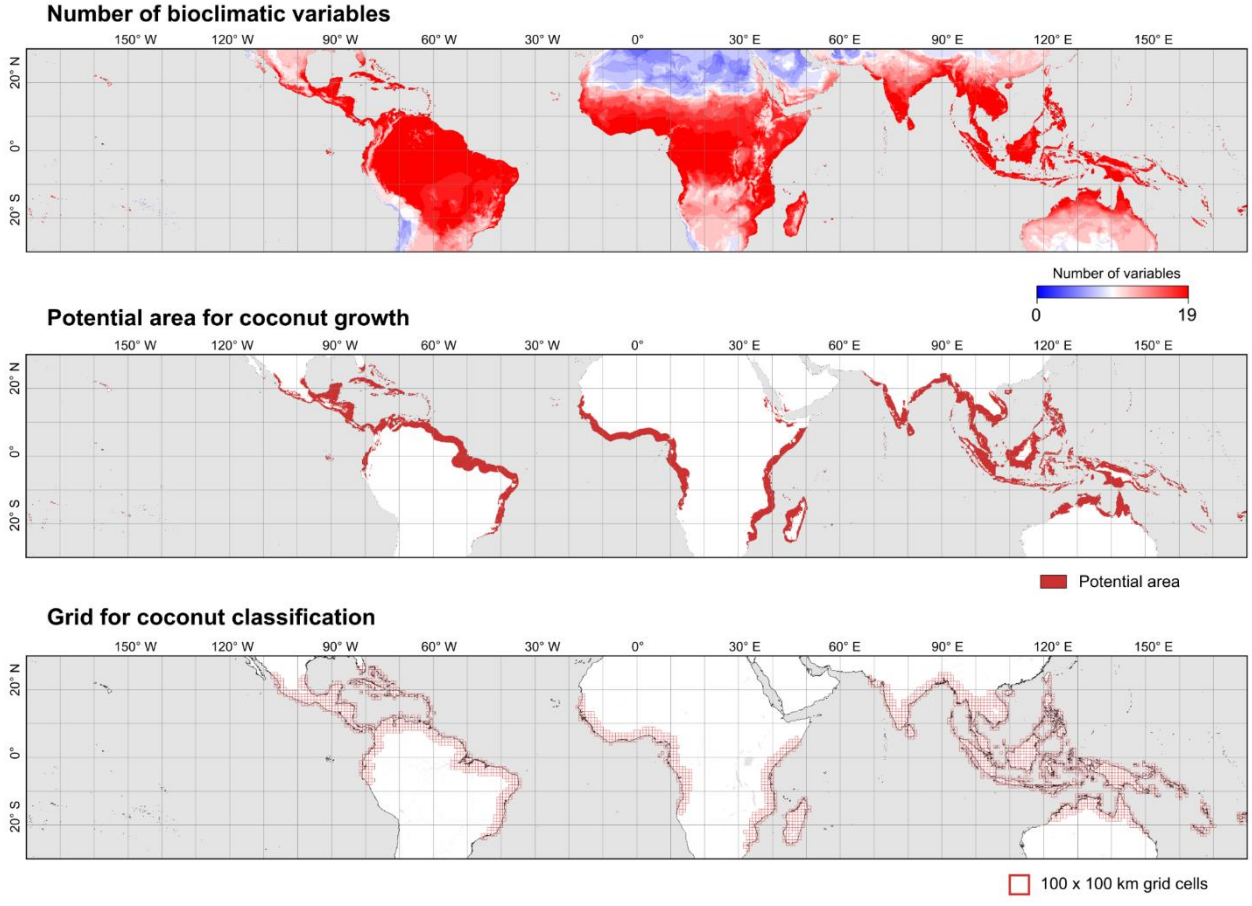

Figure A1: Maps generated from bioclimatic analysis. (a) Number of WorldClim bioclimatic variables that fall within the range of 1,139 coconut locations. (b) Potential distribution suitable for coconut growth. The map represents the pixels with at least 18 bioclimatic variables out of 19 falling within the range observed in the 1,139 coconut locations. Regions inland that are more than 200 kilometres from the coast were masked. (c) 100x100 grid used to generate the Sentinel-1 and Sentinel-2 composites.

https://doi.org/10.5194/essd-2022-463
Preprint. Discussion started: 14 February 2023

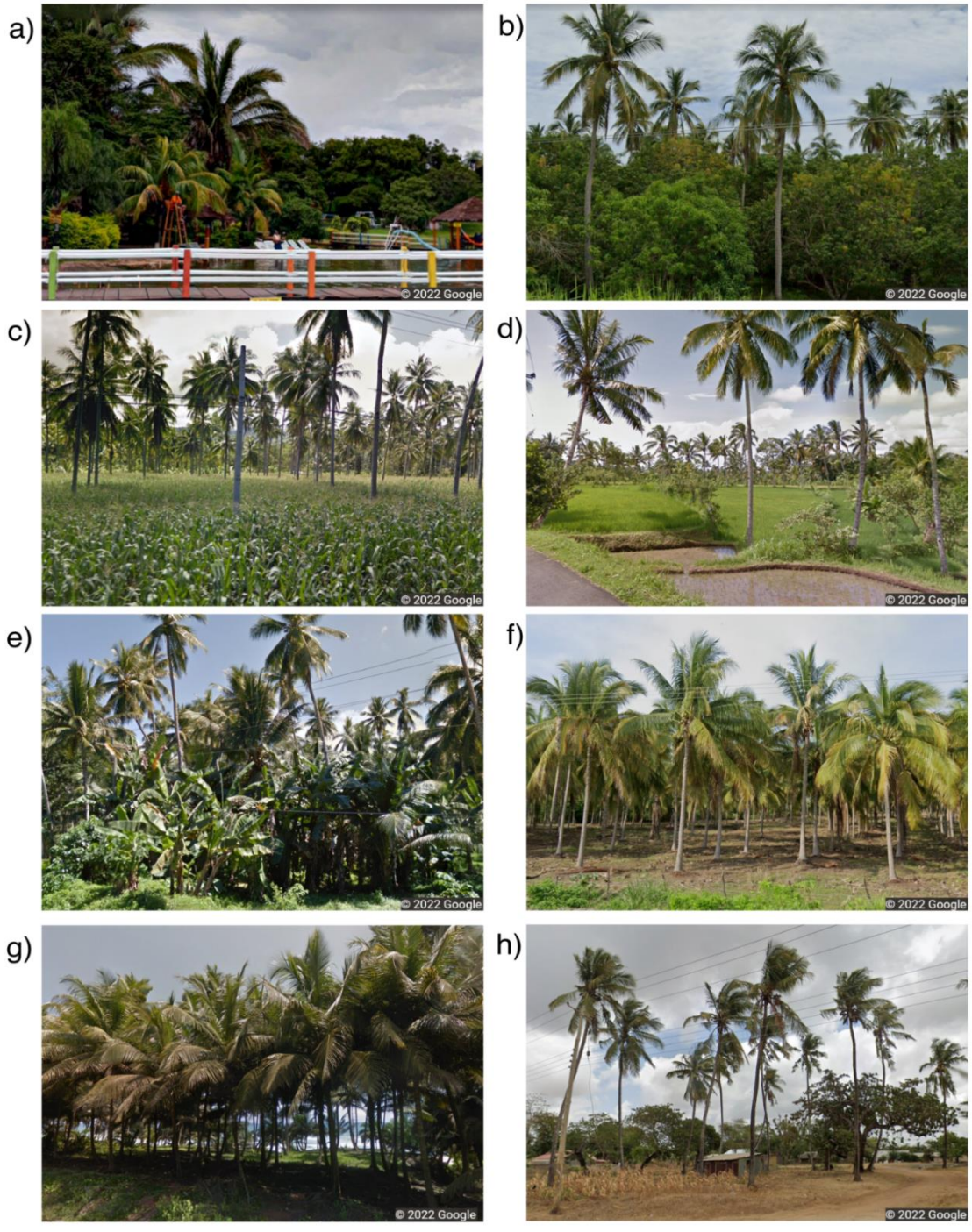

Figure A2: Images taken from Google street maps @ Google. The images show (a) two coconut trees in Bolivia at 808 km from the coast (15.9220°S, 63.1761°W), (b) an intercropping of coconut and mango in Mexico (17.2119°N, 100.7382°W), (c) coconut and maize in Philippines (5.9776°N, 124.6742°E), (d) coconut and rice in Indonesia (8.5596°S, 116.3908°E), and (e) coconut and banana in Indonesia (1.0807°S, 103.7871°E), (f) a dense coconut plantation in Mexico (18.1230°N, 102.8654°W), (g) dense coastal coconut in Indonesia (1.2783°S, 123.5367°E), and (h) sparse coconut in Kenya (3.7843°S, 39.8228°E).

https://doi.org/10.5194/essd-2022-463
Preprint. Discussion started: 14 February 2023

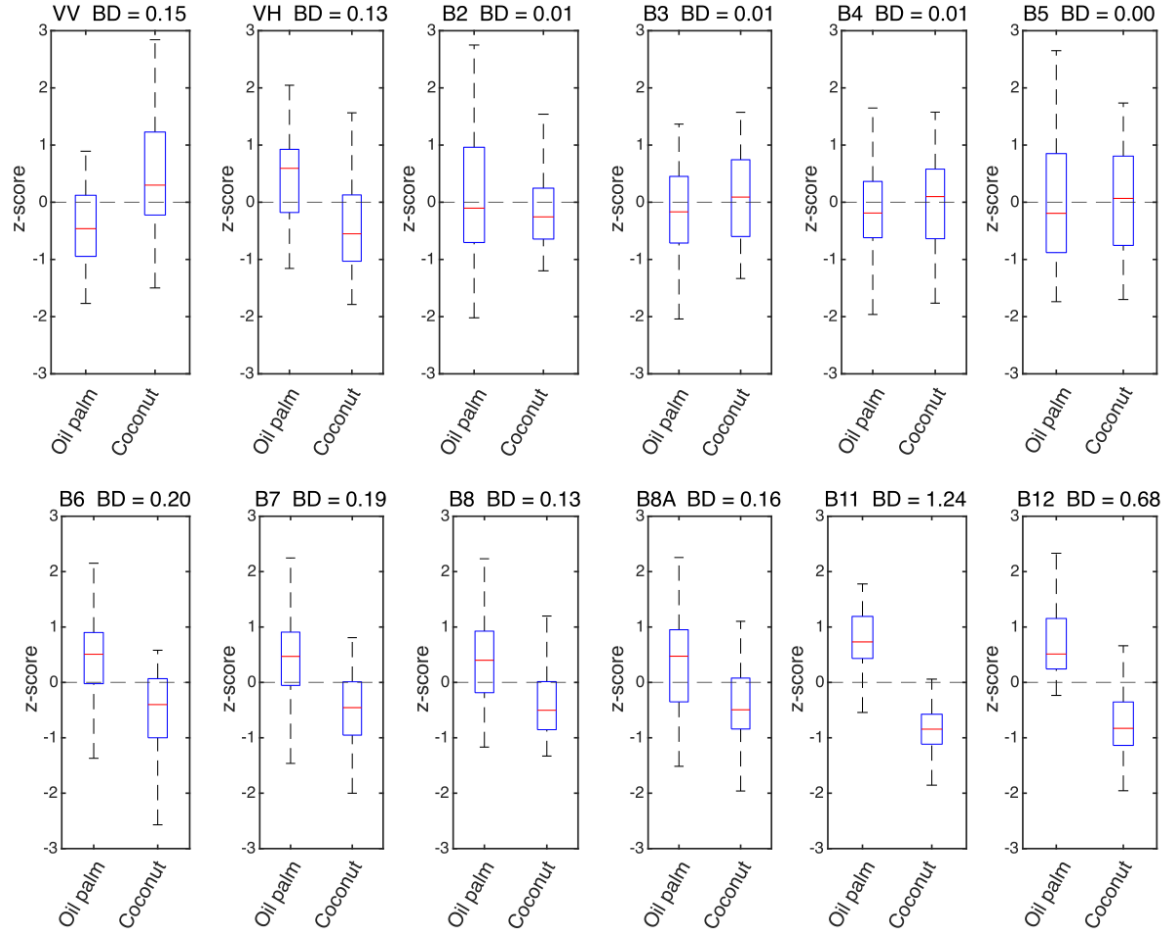

Figure A3: Spectral and backscatter separability in coconut and oil palm plantations. The overlap between distributions was estimated for the VV and VH bands in Sentinel-1 and for the 10- and 20-meter bands in Sentinel-2. The separability was measured in terms of Bhattacharyya distance (BD) between distributions of coconut and oil palm points. The higher the Bhattacharyya distance the lower the overlap between the two distributions.

https://doi.org/10.5194/essd-2022-463
Preprint. Discussion started: 14 February 2023

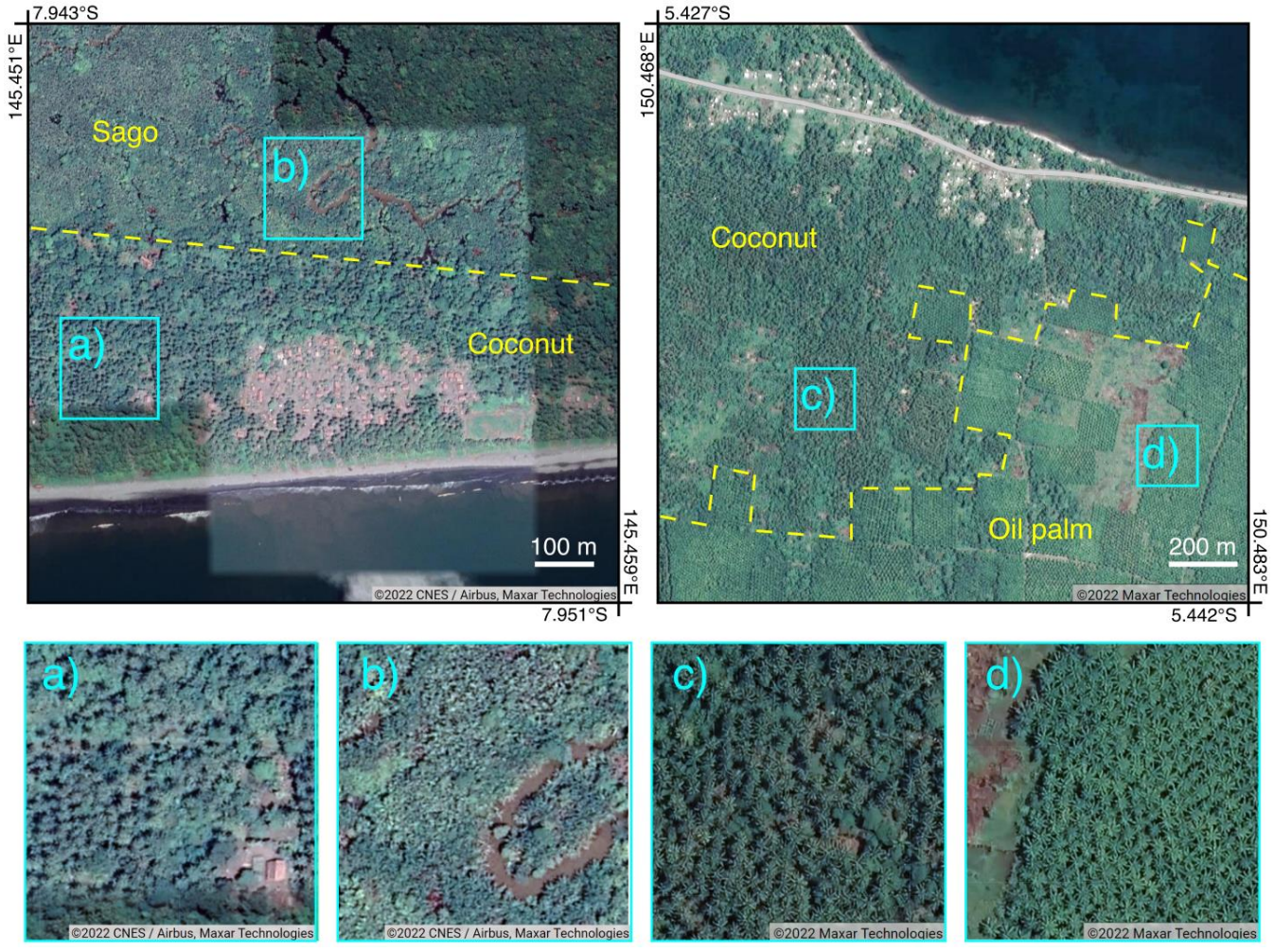

690 **Figure A4: Sub-meter resolution images in the Gulf (upper-left) and West New Britain (upper-right) provinces, Papua New Guinea. The images reveal that coconut trees and other palms (sago and oil palm) grow in separate areas. The bottom panels feature detailed images of coconut, sago, and oil palm. The satellite images are the sub-meter resolution images that are displayed as the base layer in Google Earth @ Google.**

695

700

https://doi.org/10.5194/essd-2022-463
Preprint. Discussion started: 14 February 2023

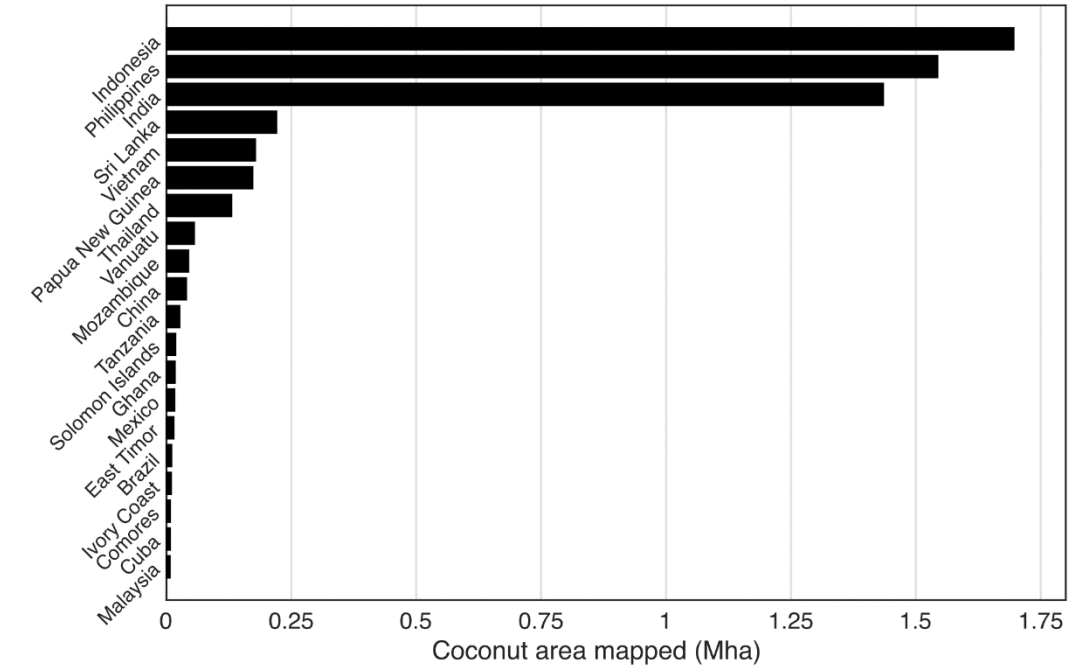

Figure A5: Coconut area mapped using Sentinel-1 and Sentinel-2 for the top 14 coconut-producing countries in 2020.

705

https://doi.org/10.5194/essd-2022-463
Preprint. Discussion started: 14 February 2023

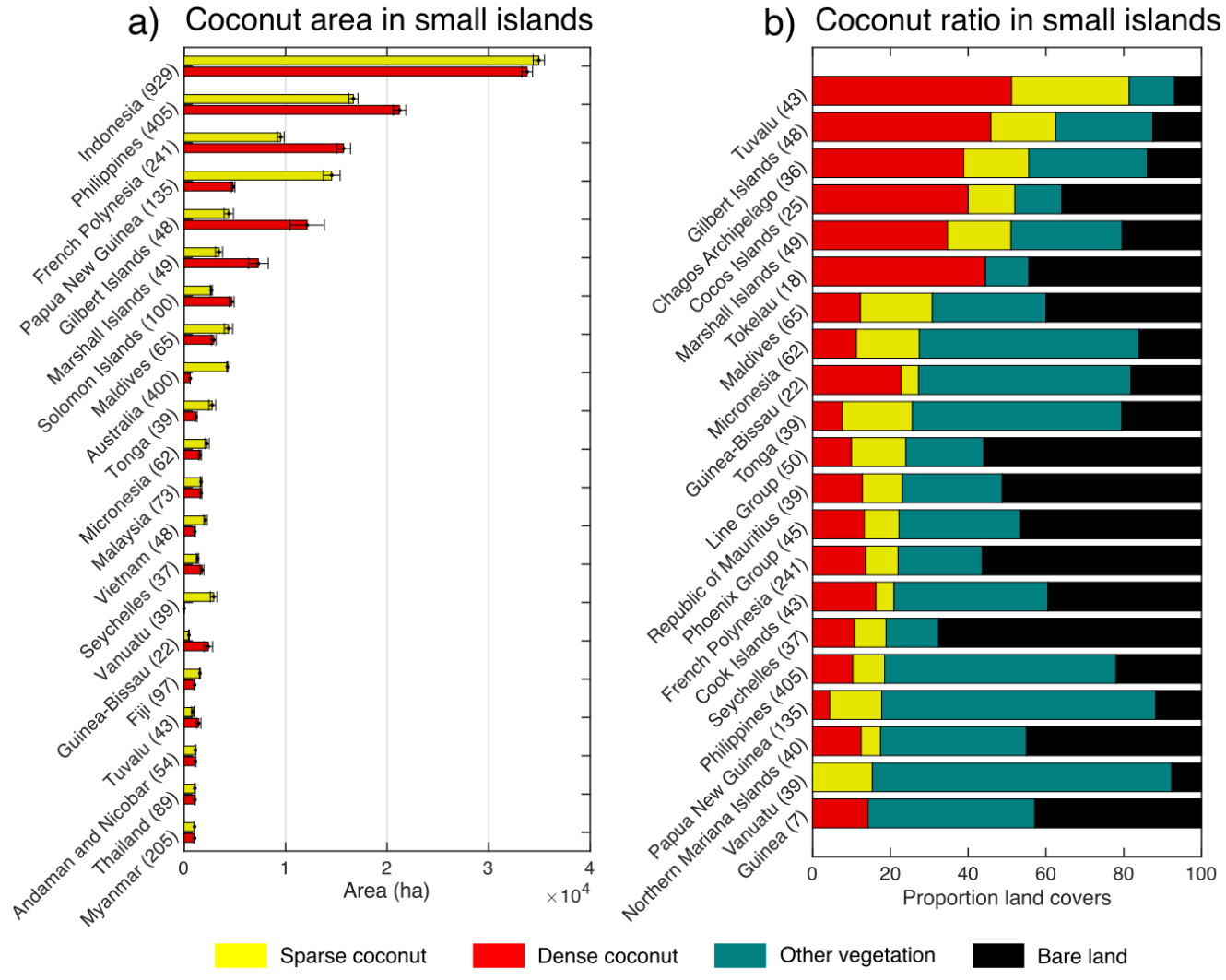

Figure A6: (a) Coconut area estimates in small tropical islands and (b) percentage of the coconut area compared to the total island surface per country. The areas and percentages were estimated using a sampling-based approach; 5,000 points were randomly sampled in small tropical islands (areas from 1 to 200 ha and between latitudes 30°S and 30°N) and the land cover was identified using sub-meter resolution images. The number between parentheses reflects the number of sampled points in each country.